Collision-Induced Dissociation of 16-mer DNA Duplexes with Various Sequences: Evidence for Conservation of the Double Helix Conformation in the Gas Phase

V. Gabelica*[†] and E. De Pauw

Mass Spectrometry Laboratory, Chemistry Institute (Bat. B6c), University of Liege, B-4000 Liege, Belgium

* Correspondence to: V. Gabelica

Tel. +32-4-366.34.32

Fax. +32-4-366.34.13

e-mail: v.gabelica@ulg.ac.be

[†] Research fellow of the F.N.R.S.

Abstract

The MS/MS of 11 different 16-mer non self-complementary DNA duplexes with various sequences has been undertaken with a quadrupole-TOF hybrid instrument. The comparison of the dissociation yields for complexes having different amounts of GC base pairs, though complicated by side-reactions like single-strand fragmentation, confirms the effect of the number of GC base pairs. More importantly, for complexes containing the same fraction of GC and different base sequences, the fragmentation yield remarkably parallels the ΔH_{diss} in solution calculated by a nearest-neighbor model for B-DNA. In addition to specific hydrogen bonding interactions, base stacking interactions also seem to survive in the gas phase and that the conformation is conserved in the gas phase. We have moreover studied the uneven partition of the negative charges between the single strands, which was found to be directed by the nature of the terminal bases exclusively, and correlated with the gas-phase acidities of the (sugar-phosphate-sugar-base) species.

Introduction

The study of non-covalent complexes by mass spectrometry has taken advantage of the introduction of electrospray (1-4), which is a soft ionization technique (4,5). Once the intact complex ions have been extracted from the solution by electrospray, they are isolated from the influence of the solvent, and their gas phase properties can be studied. The dissociation of the so-produced complexes is induced in the gas phase by collisions at different energies, and the dissociation products are analyzed by tandem mass spectrometry. The literature concerning ESI-MS/MS of non-covalent complexes is constantly growing (6-10), and one of the major current issues is whether the gas-phase and the solution phase structures are related to each other. How soft is the transfer of weak complexes from the solution to the gas phase? Can extensive rearrangements occur upon removal of the solvent, or is the solution-phase structure “trapped” in a potential energy minimum?

It has been shown in several papers that the electrostatic and hydrogen bonding interactions initially present in solution remain in the gas-phase complexes (11-13), as they are strengthened in the absence of solvent. Strongly solvent-dependent interactions like hydrophobic interactions are however suppressed in the gas phase. The gas-phase kinetic and thermodynamic stability can therefore be totally different from that in solution in cases where hydrophobic interactions are predominant in solution (12,14). In the case of weak, short-range (and therefore strongly conformation-dependent) interactions like dipole-dipole, dipole-induced dipole and van der Waals interactions, their possible conservation in the gas phase upon electrospray transfer is still a debatable point (10).

We recently reported some preliminary results of source-CID of DNA duplexes suggesting that, in addition to hydrogen bonding interactions, base stacking interactions could also be conserved in the gas phase (15). Three kinds of interactions are involved in the formation of the DNA double helix (16-18). Phosphate groups are negatively charged, and electrostatic interactions, strongly dependent on the ionic strength of the solution, are important: the concentration of counter-ions needs to be high enough to counterbalance the charges of the phosphates, unless the two strands would separate because of charge repulsion. The purine and pyrimidine bases interact with each other by hydrogen bonding in the so-called Watson-Crick base pairing motif. The correlation between the fraction of GC base pairs and the gas-phase kinetic stability has been already reported by different authors (15,19-21), suggesting that the Watson-Crick base pairing is conserved in the gas phase. Finally, adjacent bases are also interacting with each other electrostatically (dipole-dipole, short range interactions) and these interactions are favored in the double helix for conformational reasons. This kind of interaction is called “base stacking” (22) and is sequence-dependent. Here we present a more extensive MS/MS study of complexes of various sequences that strongly indicates that base stacking short-range interactions are conserved in the gas-phase duplexes. The assumptions used for the comparison of kinetic stabilities in the gas phase and energetic stabilities in solution have been discussed previously (15) and we compared complexes of the same size (16-mers) to avoid any degrees-of-freedom effects. We also studied the partition of the charges between the single strands upon dissociation of the duplex, and show that the terminal bases are directing the uneven partition of the charges.

Experimental Section

All oligonucleotides were purchased from Eurogentec (Sart-Tilman, Belgium) and used without further purification. Stock solutions of 50 µM duplex (noted AB) were prepared by heating the strands A and B to 75 °C and cooling overnight. Annealing was performed in 50 mM aqueous ammonium acetate. A solution of 20 µM duplex in 20:80 (v/v) methanol/50 mM aqueous NH_4OAc, was injected in the mass spectrometer with a Harvard pump (model 22) at the flow rate of 5 µL/min.

The MS/MS experiments were performed on a Q-TOF2 (Micromass, Manchester, UK) electrospray mass spectrometer, and the Z-spray source was operated in the negative ion mode at a capillary voltage of –2350 V. The source block temperature was 80 °C and the desolvation gas (N_2) temperature was 100 °C. The collisions with argon in the second quadrupole were conducted at different collision energies so as to follow the dissociation of the duplex from 100% to 0% of relative abundance. The relative abundance of duplex^{6-} was calculated with equation (1).

$$\%\text{Duplex}=\frac{I(AB^{6-})}{I(AB^{6-})+\frac{I(A^{3-})+I(B^{3-})}{2}}.100\% \qquad (1)$$

This intensity ratio may not reflect the true ion ratio as the MCP detector efficiency varies with the charge on the ion, but the current method is adequate for comparisons between complexes of the same charge state. Intensities were measured after a double smoothing of each spectrum over a 4-channel window (approx. 0.1 m/z in the mass range of interest).

Results and Discussion

1. Influence of the charge state on the dissociation profile

Figure 1 shows the MS/MS spectra of the AB duplex 50%-2 (see table 1 for complete sequence of strands A and B) for the charge states 8-, 7-, 6- and 5-. The ease of fragmentation depends on the number of charges on the duplex, due to Coulombic repulsion. Duplex^{8-} fragments in three competing ways: (1) each strand takes 4 charges, (2) strand A keeps 5 charges and strand B keeps 3 charges or (3) strand A keeps 3 charges and strand B, 5 charges. For duplex^{7-}, the charges are spread on the two strands, and there are two possible dissociation channels:

$$AB^{7-} \xrightarrow{\mathbf{a}} A^{3-} + B^{4-} \qquad AB^{7-} \xrightarrow{\mathbf{b}} A^{4-} + B^{3-} \tag{2}$$

As in the case of duplex^{8-}, the two strands do not have the same tendency to keep the negative charges. This feature will be discussed in the next section. For duplex^{6-}, the charges are evenly distributed (A^{3-} + B^{3-}), and the energy necessary to induce the dissociation is still higher. For duplex^{5-}, covalent fragmentation of the single strands and base loss occur instead. The dissociation into single strands is favored by the Coulombic repulsion between the strands. If the Coulombic repulsion diminishes, the threshold for noncovalent dissociation diminishes, and the energy required to break the complex increases (cove voltage of 45 V and collision energy of 30 eV for AB^{5-}). The single strands issued from the dissociation contain enough excess energy to

fragment further into [w] and [a-B] ions. The base loss from the duplex is also a low-threshold process that can occur when the dissociation threshold is high (20). The competition between non-covalent dissociation and covalent fragmentation will be discussed in detail elsewhere (Gabelica and De Pauw, submitted for publication).

2. Uneven distribution of the negative charges

The uneven distribution of the charges was studied in detail for the 11 duplexes by performing MS/MS on the complexes with seven negative charges. This uneven charge state has been chosen because of the simplicity of the resulting spectra: only the two dissociation channels of interest are seen, and no fragmentation of the single strands occurs. In figure 2 are displayed the MS/MS spectra of two duplexes containing 25% of GC base pairs each, differing only in the position of the bases (see table 1 for the complete sequence description). For duplex 25%-1, strand B has a greater tendency to keep negative charges, whether for duplex 25%-2, it is strand A that has a tendency to keep more negative charges. The same measurements have been performed for all duplexes. For all of them the proportion of the two dissociation channels does not change when increasing the collision energy. The mean proportion of channel **a** (see definition in equation 2) is calculated with equation 3. The results are summarized in table 1.

$$\% \text{ Channel } \mathbf{a} = \frac{I(A^{3-})+I(B^{4-})}{I(A^{3-})+I(B^{4-})+I(A^{4-})+I(B^{3-})}.100\% \qquad (3)$$

In a previous publication (23), we mentioned that upon MS/MS, the duplex $[d(GGGGATATGGGG).d(CCCCATATCCCC)]^{5-}$ fragmented with 3 charges preferably on the G-rich strand. This was correlated with the pKa of guanine, that is superior to that of cytosine. The greater amount of results reported here allow to refine our understanding of the phenomenon. When examining table 1 in detail, we can find no direct correlation between the propensity to take more negative charges and the number of a particular base contained in the strands. Rather, these are mainly the terminal bases that seem to govern the fragmentation channel. If strand A

(B) has an adenine (thymine) at each end, channel **a** will be preferred (see duplex 0%-1, 25%-1 and 50%-1). If strand A (B) has a guanine (cytosine) on each strand, channel **b** will be preferred (see duplex 25%-2, 50%-2, 50%-4, 75%-3, 100%-1). Two duplexes (50%-3 and 73%-1) have a guanine at one end of strand A and an adenine at the other end; no dissociation channel is markedly preferred. Only the difference between duplexes 75%-2 and 75%-3 cannot be accounted for, as the two duplexes differ only by the position of the four central A/T bases. With the set of sequences studied here, it is not possible to assess whether the 5’ or 3’ location of the bases is a key factor for determining the distribution of the charges on the strands.

As a general rule, the negative charges therefore remain preferentially on the strands that bear guanine rather than cytosine, or thymine rather than adenine at the extremities. First, a correlation was sought with the pKa’s (23) (or better, the gas-phase acidities) of the bases, it accounts for the guanine/cytosine ranking order, but not for adenine/thymine. However, a good agreement with our observations is found if the gas phase acidities of the [sugar-phosphate-sugar-base] species are considered (see table 3 of reference (24)), as the charge is located on the phosphate groups of the strands, not on the bases. The fact that the terminal base pairs are of prime importance for the distribution of the charges on the fragments is also consistent with the Coulombic repulsion that forces the charges apart to the terminal phosphodiester groups (25).

3. Persistence of weak, highly conformation-dependent interactions in the gas phase

Base stacking interactions in solution translate into a sequence-dependent stability of oligonucleotide duplexes. Nearest-neighbor (n-n) models (18) are established to calculate the sequence-dependent stability of short duplex DNA oligomers (20 base pairs or less). They are based on the statistical analysis of denaturation (melting) data and provide tables that can be used to calculate thermodynamic parameters for any sequence by an incremental method. We used the tables given by Sugimoto et al. (26) to calculate the duplex melting enthalpy (ΔH_{n-n}) that will be correlated with the gas-phase kinetic stability measured by MS/MS. This kinetic stability has been measured for duplex 6- and 7-, and the results are similar (data for duplex^{7-} not shown). The percentage of surviving duplex^{6-} was determined with equation 1 and is plotted against the collision energy in figures 3-5, for duplexes containing different percentages of GC base pairs. The comparison of these three figures confirms that a higher collision energy is necessary to fragment duplexes containing more hydrogen bonds, but this is not the only factor determining the gas-phase stability of the duplexes. The ΔH_{n-n} values (calculated from table III-D in reference 18) related to each duplex are gathered in the insets of the relevant figures. Only complexes of the same percentage of GC base pairs are compared on a given figure in order to have the same number of hydrogen bonds and enlighten only the effect of stacking interactions.

Figure 3 displays the results obtained for the 2 duplexes with 25% of GC base pairs. There is a marked difference in their gas-phase kinetic stabilities that parallels their respective stabilities in solution. The same tendency is observed for the dissociation of the duplex^{7-}: in figure 2, the MS/MS spectra of both duplexes at the same collision energy also show that duplex 25%-1 is

more kinetically stable than duplex 25%-2. Figure 4 gathers the results for 4 duplexes with 50% GC. For the first three duplexes the gas-phase stabilities also parallel those calculated by nearest-neighbor models. Only duplex 50%-4 (sequence d(GGGCTTTTAAAACGGG)) does not obey this rule. This exception can be explained by the fact that, in solution, A-tract cause significant curvature of the B-DNA structure that is locally distorted (27-30). The nearest-neighbor models, that are applicable to B-DNA only, are therefore not suitable to calculate the solution-phase stability of these special structures that are less stable than if they were B-DNA's. The lower gas-phase kinetic stability observed for this duplex may indicate this distorted structure is conserved in the gas phase. For the three duplexes with 75% GC base pairs (figure 5), the correlation between the solution and gas-phase stabilities is also qualitatively excellent. It must be noted that in the present case the %Duplex calculated with equation (1) is approximate for collision energies equal or higher than 30 eV due to the competition between noncovalent dissociation and covalent bond cleavage of the single strands.

In summary, the results clearly suggest that the weak base stacking interactions that are responsible for the sequence-dependent stability in solution are conserved in the gas phase. As these interactions are short-range and very conformation-dependent, the double helix structure must not be perturbed during the electrospray transfer process in order for these interactions to be kept in the gas phase.

Acknowledgements

VG is grateful to the F.N.R.S. for a research fellowship. This work is supported by the “Actions de Recherche Concertée” (ARC) (Direction de la Racherche Scientifique, Communauté Française de Belgique).

References

1 M. Yamashita and J.B. Fenn, J. Phys. Chem., 88 (1984) 4451.

2 M. Whitehouse, R.N. Dreyer, M. Yamashita, and J.B. Fenn, Anal. Chem., 57 (1985) 675.

3 J.B. Fenn, M. Mann, C.K. Meng, S.F. Wong, and C.M. Whitehouse, Science, 246 (1989) 64.

4 J.B. Fenn, M. Mann, C.K. Meng, and S.F. Wong, Mass Spectrom. Rev., 9 (1990) 37.

5 C. Collette and E. De Pauw, Rapid Commun. Mass Spectrom., 12 (1998) 165.

6 R.D. Smith and K.J. Light-Wahl, Biol. Mass Spectrom., 22 (1993) 493.

7 M. Przybylski and M.O. Glocker, Angew. Chem. Int. Ed. Engl., 35 (1996) 806.

8 J.A. Loo, Mass Spectrom. Rev., 16 (1997) 1.

9 R.D. Smith, J.E. Bruce, Q. Wu, and Q.P. Lei, Chem. Soc. Rev., 26 (1997) 191.

10 S.A. Hofstadler and R.H. Griffey, Chem. Rev., 101 (2001) 377.

11 Q. Gao, X. Cheng, R.D. Smith, C.F. Yang, and I.H. Goldberg, J. Mass Spectrom., 31 (1996) 31.

12 H. Rogniaux, A. Van Dorsselaer, P. Barth, J.F. Biellmann, J. Brabanton, M. van Zandt, B. Chevrier, E. Howard, A. Mitschler, N. Potier, L. Urzhumtseva, D. Moras, and A. Podjarny, J. Am. Soc. Mass Spectrom., 10 (1999) 635.

13 J. Gao, Q. Wu, J.D. Carbeck, Q.P. Lei, R.D. Smith, and G.M. Whitesides, Biophys. J., 76 (1999) 3253.

14 Q. Wu, J. Gao, D. Joseph-McCarthy, G.B. Sigal, J.E. Bruce, G.M. Whitesides, and R.D. Smith, J. Am. Chem. Soc., 119 (1997) 1157.

15 V. Gabelica and E. De Pauw, J. Mass Spectrom., 36 (2001) 397.

16 K.A. Sharp and B. Honig, Curr. Opin. Struct. Biol., 5 (1995) 323.

17 D.H. Turner, Curr. Opin. Struct. Biol., 6 (1996) 299.

18 R. Owczarzy, P.M. Vallone, F.J. Gallo, T.M. Paner, M.J. Lane, and A.S. Benight, Biopolymers, 44 (1998) 217.

19 D.C. Gale and R.D. Smith, J. Am. Soc. Mass Spectrom., 6 (1995) 1154.

20 P.D. Schnier, J.S. Klassen, E.F. Strittmatter, and E.R. Williams, J. Am. Chem. Soc., 120 (1998) 9605.

21 K.X. Wan, T. Shibue, and M.L. Gross, J. Am. Soc. Mass Spectrom., 11 (2000) 450.

22 J. Sponer, J. Laszczynski, and P. Hobza, J. Biomol. Struct. Dyn., 14 (1996) 117.

23 V. Gabelica, E. De Pauw, and F. Rosu, J. Mass Spectrom., 32 (1999) 1328.

24 S. Habibi-Goudarzi and S.A. McLuckey, J. Am. Soc. Mass Spectrom., 6 (1995) 102.

25 A. Favre, F. Gonnet, and J.C. Tabet, Eur. J. Mass Spectrom., 6 (2000) 389.

26 N. Sugimoto, S.-I. Nakano, M. Yoneyama, and K.-I. Honda, Nucl. Acid. Res., 24 (1996) 4501.

27 D. MacDonald, K. Herbert, X. Zhang, T. Polgruto, and P. Lu, J. Mol. Biol., 306 (2001) 1081.

28 D. Strahs and T. Schlick, J. Mol. Biol., 301 (2000) 643.

29 R.P. Ojha, M.M. Dhingra, M.H. Sarma, M. Shibata, M. Farrar, C.J. Turner, and R.H. Sarma, Eur. J. Biochem., 265 (1999) 35.

30 M.A. Young, J. Srinivasan, I. Goljer, S. Kumar, D.L. Beveridge, and P.H. Bolton, Methods Enzymol., 261 (1995) 121.

Figure Legends

Figure 1.

MS/MS on different charge states of duplex 50%-2: (a) on duplex^{8-} with 12 eV collision energy (cone voltage = 17 V), (b) on duplex^{7-} with 14 eV collision energy (cone voltage = 20 V), (c) on duplex^{6-} with 20 eV collision energy (cone voltage = 30 V) and (d) on duplex^{5-} with 30 eV collision energy (cone voltage = 45 V). The duplex is noted AB (see table 1 for the complete sequences of strands A and B). The peaks marked with stars are sodium adducts.

Figure 2.

MS/MS spectra of duplexes 25%-1 (top) and 25%-2 (bottom) (see table 1 for detailed base sequences) at 12 eV collision energy.

Figure 3.

Dissociation curves for the 2 duplexes containing 25% of GC base pairs. The % Duplex is calculated with equation 1 for each collision energy. The cone voltage was set to 20 V. The corresponding solution melting enthalpies are written in the inset, together with the number of the oligo (see table 1 for detailed base sequences).

Figure 4.

Dissociation curves for the 4 duplexes containing 50% of GC base pairs. The % Duplex is calculated with equation 1 for each collision energy. The cone voltage was set to 20 V. The corresponding solution melting enthalpies are written in the inset, together with the number of the oligo (see table 1 for detailed base sequences).

Figure 5.

Dissociation curves for the 3 duplexes containing 75% of GC base pairs. The % Duplex is calculated with equation 1 for each collision energy. The cone voltage was set to 20 V. The corresponding solution melting enthalpies are written in the inset, together with the number of the oligo (see table 1 for detailed base sequences).

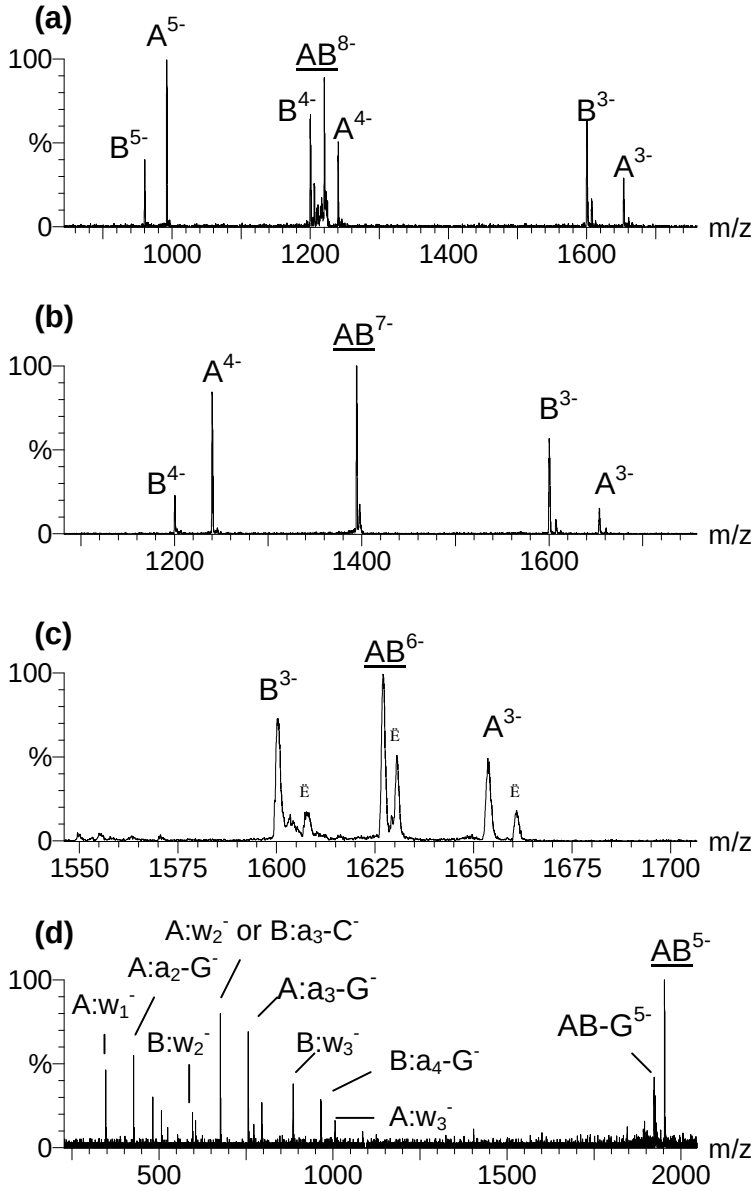
(a)
100
%
0
A5-
AB8-
B4-
A4-
B5-
B3-
A3-
1000
1200
1400
1600
m/z
(b)
100
%
0
AB7-
A4-
B3-
B4-
A3-
1200
1400
1600
m/z
(c)
100
%
0
AB6-
B3-
A3-
1550
1575
1600
1625
1650
1675
1700
m/z
(d)
100
%
0
A:w2- or B:a3-C-
A:a2-G-
A:a3-G-
A:w1-
B:w2-
B:w3-
B:a4-G-
A:w3-
AB5-
AB-G5-
500
1000
1500
2000
m/z

Figure 1.

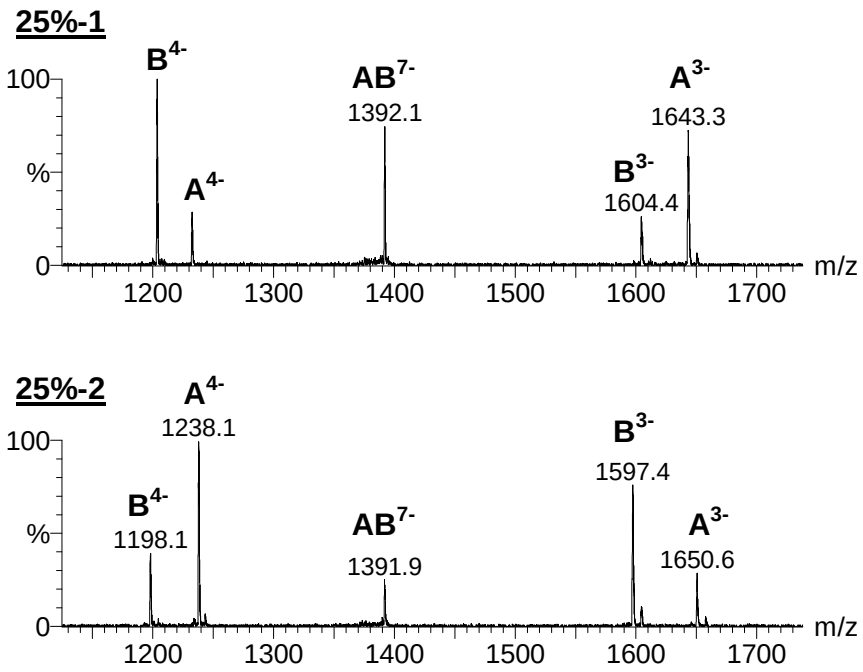
25%-1
B4-
AB7-
1392.1
A3-
1643.3
B3-
1604.4
A4-
100
%
0
1200
1300
1400
1500
1600
1700
m/z
25%-2
A4-
1238.1
B3-
1597.4
B4-
1198.1
AB7-
1391.9
A3-
1650.6
100
%
0
1200
1300
1400
1500
1600
1700
m/z

Figure 2.

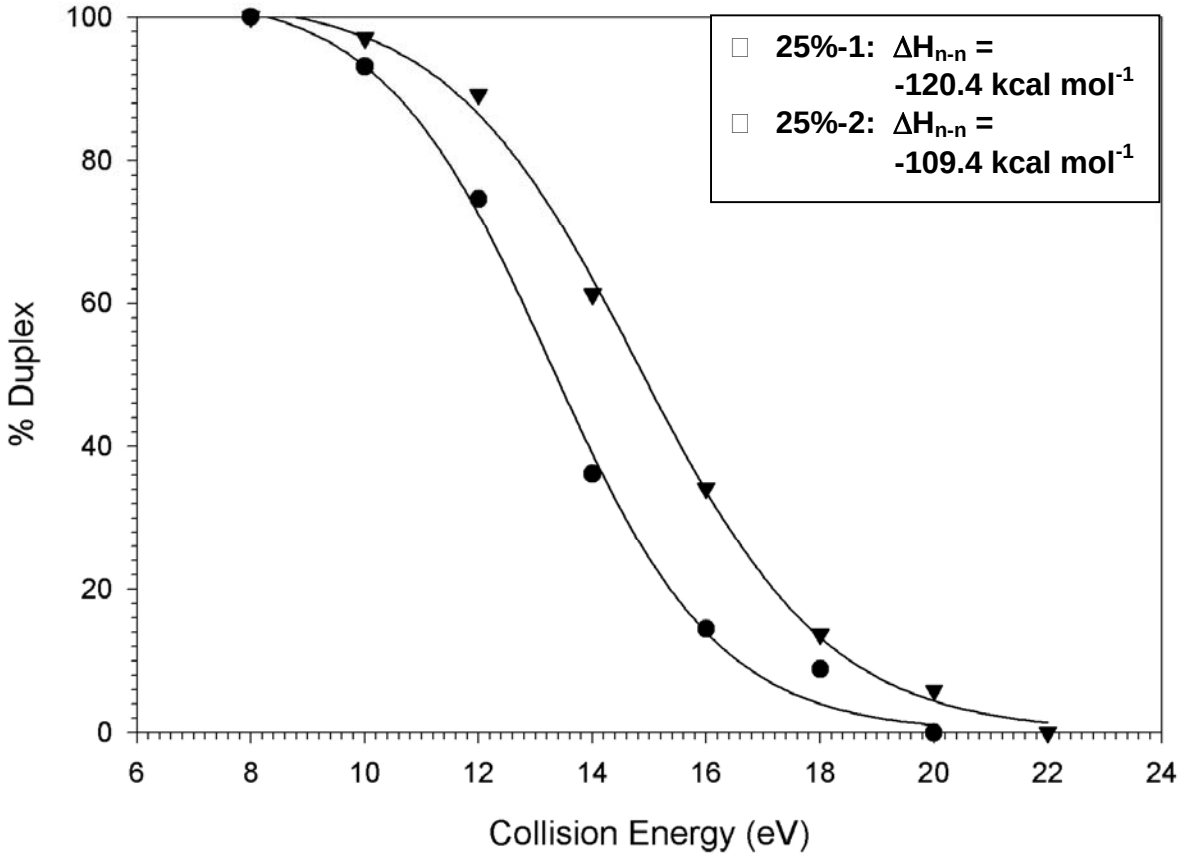
100
80
60
40
20
0
% Duplex
6
8
10
12
14
16
18
20
22
24
Collision Energy (eV)
25%-1: ΔHn-n = -120.4 kcal mol-1
25%-2: ΔHn-n = -109.4 kcal mol-1

Figure 3.

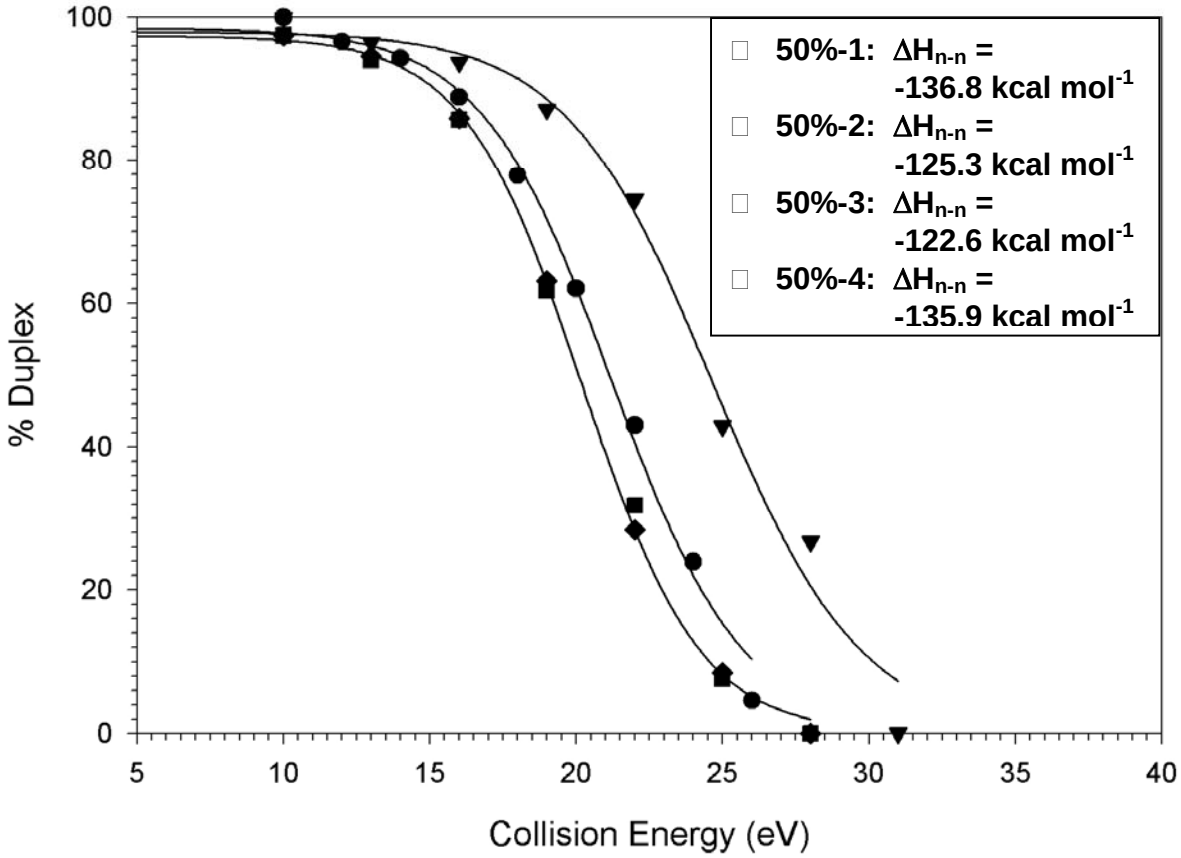
100
80
60
40
20
0
% Duplex
5
10
15
20
25
30
35
40
Collision Energy (eV)
50%-1: ΔHn-n = -136.8 kcal mol-1
50%-2: ΔHn-n = -125.3 kcal mol-1
50%-3: ΔHn-n = -122.6 kcal mol-1
50%-4: ΔHn-n = -135.9 kcal mol-1

Figure 4.

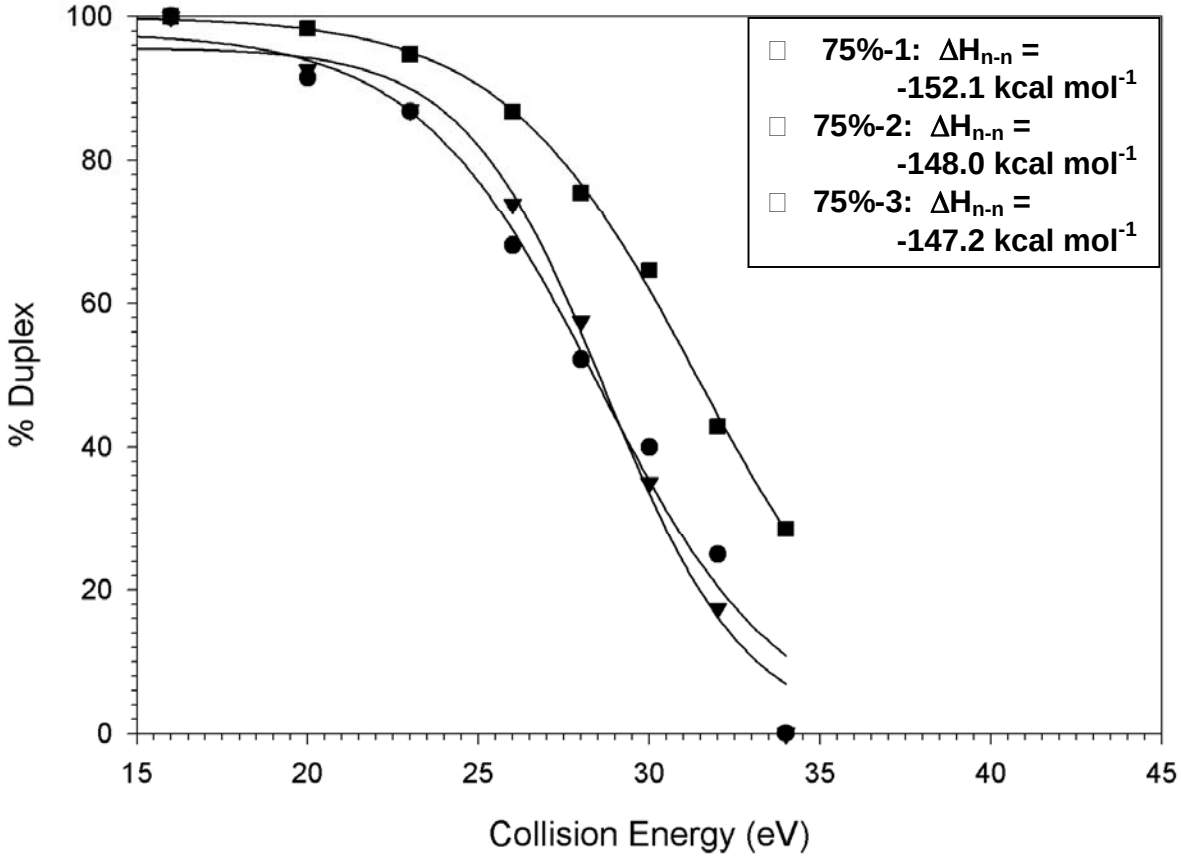
100
80
60
40
20
0
% Duplex
15
20
25
30
35
40
45
Collision Energy (eV)
75%-1: ΔHn-n = -152.1 kcal mol-1
75%-2: ΔHn-n = -148.0 kcal mol-1
75%-3: ΔHn-n = -147.2 kcal mol-1

Figure 5.

Table 1. Base sequences of the studied duplexes, and measured proportion of dissociation channel **a** (A^{3-} + B^{4-}).

No.	Strand	Sequence	Proportion of channel **a**[a]
0%-1	A:	5’-AAATTATAATATTAAA-3’	83 %
	B:	3’-TTTAATATTATAATTT-5’	
25%-1	A:	5’-AAATTAGCGGATTAAA-3’	75 %
	B:	3’-TTTAATCGCCTAATTT-5’	
25%-2	A:	5’-GGATTATAATATTAGG-3’	30 %
	B:	3’-CCTAATATTATAATCC-5’	
50%-1	A:	5’-AAATCGCGGCGCTAAA-3’	71 %
	B:	3’-TTTAGCGCCGCGATTT-5’	
50%-2	A:	5’-GGGCTATAATATCGGG-3’	21 %
	B:	3’-CCCGATATTATAGCCC-5’	
50%-3	A:	5’-AGACTGTGAGTCAGTG-3’	53 %
	B:	3’-TCTGACACTCAGTCAC-5’	
50%-4	A:	5’-GGGCTTTTAAAACGGG-3’	34 %
	B:	3’-CCCGAAAATTTTGCCC-5’	
75%-1	A:	5’-AATTCGCGGCGCCGGG-3’	55 %
	B:	3’-TTAAGCGCCGCGGCCC-5’	
75%-2	A:	5’-GGGCCGAATTGCCGGG-3’	48 %
	B:	3’-CCCGGCTTAACGGCCC-5’	
75%-3	A:	5’-GGGCCGTAATGCCGGG-3’	35 %
	B:	3’-CCCGGCATTACGGCCC-5’	
100%-1	A:	5’-GGGCCGCGGCGCCGGG-3’	41 %
	B:	3’-CCCGGCGCCGCGGCCC-5’	

a. Calculated with equation 3.